Itinerant origin of the ferromagnetic quantum critical point in Fe(Ga,Ge)₃

David J. Singh

Materials Science and Technology Division, Oak Ridge National Laboratory, Oak Ridge, Tennessee 37831-6056, USA

The electronic structure and magnetic properties of $FeGa_3$ and doped $FeGa_3$ are studied using density functional calculations. An itinerant mechanism for ferromagnetism is found both for n-type doping with Ge and also for p-type doping. Boltzmann transport calculations of the thermopower are also reported.

I. INTRODUCTION

$FeGa_3$ is a tetragonal semiconductor with a band gap of ~ 0.5 eV,[1] and interesting thermoelectric properties. These include a high thermopower when doped,[2–4] although high figures of merit ZT have not been realized due to the combination of thermal and electrical conductivities. The compound shows diamagnetic behavior, but, remarkably, when modestly electron doped by Ge, a ferromagnetic quantum critical point emerges and the ground state becomes a ferromagnetic metal.[5,6] Such quantum critical systems can show unconventional and sometimes remarkable physical properties, especially if the magnetic system is strongly coupled to itinerant electrons and if the itinerant electrons are heavy. From an experimental point of view, $FeGa_3$ does show evidence that it is in this regime from transport, specific heat, and other measurements.[5,7,8] For example, Umeo and co-workers report a specific heat γ of 70 mJ K^{-2} per mole for $FeGa_{3-y}Ge_y$, $y = 0.09$, while the thermopower $S(T)$, as mentioned, is large, e.g., $S(300) \sim -400 - -560$ μV/K for n-type carrier concentrations in the 10^{18} cm^{-3} range.[2–4] We note that the electrons at the Fermi energy and their excitations govern transport as well as low-energy thermodynamic properties such as specific heat and the enhanced Pauli part of the susceptibility. Since these are strongly coupled to the magnetic order parameter and fluctuations in itinerant magnets, strong signatures of quantum criticality may be expected, and in fact, this appears to be the case in some materials, as discussed, for example, in Refs. 9 and 10.

Several density functional theory (DFT) studies using standard functionals (with no additional correlation term, such as U in LDA $+ U$ calculations) have shown that the band gap of $FeGa_3$ is well described without magnetism on the Fe and without strong correlation effects.[1,11–14] However, Yin and Pickett also reported calculations with an additional interaction U in LDA $+ U$ calculations.[12] They observed that at modest values of $U - J = 1.4$ eV (J is the Hund's parameter in the LDA $+ U$ calculations, the dependence is on $U - J$) an antiferromagnetic state appears, with moments somewhat below 1 μ_B, which is the spin-1/2 value. It has subsequently been argued that the observed magnetism in doped $FeGa_3$ is related to these moments, specifically that the additional carriers break up singlets formed by spin-1/2 Fe dimers in the structure leading to free spins that order ferromagnetically.[6] This picture involving spin-1/2 dimers suggests some similarity to VO_2, where the relationship between this structural feature and the electronic structure has been discussed by Eyert.[15,16]

There are some questions related to this explanation. First of all, the undoped compound is diamagnetic below room temperature,[1,3,17] and the susceptibility shows an increase above room temperature consistent with free carriers generated for a band gap in accord with the measured band gap.[17] Second, ^{57}Fe Mossbauer spectra show no magnetism in the undoped compound. Third, the thermoelectric transport properties of $RuGa_3$ and $OsGa_3$ indicate similar behavior to $FeGa_3$ allowing for carrier concentration differences;[2,18] this indicates a similar electronic structure. Finally, while Yin and Pickett[12] indicate that they obtain qualitatively similar behavior and predictions independent of the $+ U$ double counting scheme [i.e., fully localized limit (FLL or SIC)) or around mean field (AMF)], Osorio-Guillen and co-workers[13] report that they find no local moments with an optimized double counting scheme intermediate between these limits.

Here we present first-principles calculations showing that the magnetism of doped $FeGa_3$ can be readily explained in an itinerant picture without the need for preexisting moments in the semiconducting state and without the need for correlation terms. We also present Boltzmann transport calculations of the thermopower and a resolution of the differences between the results of Yin and Pickett[12] and those of Osorio-Guillen and co-workers.[13]

II. COMPUTATIONAL DETAILS

The present calculations were performed within density functional theory using the generalized gradient approximation of Perdew, Burke, and Ernzerhof (PBE).[19] For this purpose, we used the general potential linearized augmented plane wave (LAPW) method[20] as implemented in the WIEN2K code.[21] We used LAPW sphere radii of 2.05 Bohr for both Fe and Ga, with highly converged basis sets. We used the standard LAPW basis set with additional local orbitals rather than the more efficient but potentially less accurate APW $+$ lo method. We did calculations both in a scalar relativistic approximation and also including spin orbit. We did not find significant differences between these. We also did GGA $+ U$ calculations both with the fully localized limit (SIC) double counting and the around mean field (AMF) double counting. For consistency, the GGA $+ U$ results discussed here were also done with the PBE GGA.

We used the experimental crystal structure, i.e., tetragonal $P4_2/mnm$, $a = 6.2628$ Å, $c = 6.5546$ Å, Fe at $(0.3437,0.3437,0)$, Ga1 at $(0,0.5,0)$, Ga2 at $(0.1556,0.1556,0.262)$, and four formula units per unit cell.

Each Fe atom in this structure has eight Ga neighbors at distances between 2.36 and 2.50 Å, which is an arrangement that is not favorable for strong d bonding, as well as one nearby Fe atom at ~2.77 Å. These relatively short-bonded Fe-Fe pairs are the dimers discussed by Yin and Pickett.[12] Interestingly, the calculated forces on the atoms were zero to the precision of the calculation (largest force was below 2 mRy/Bohr in scalar relativistic calculations) for this structure. This is in contrast to the Fe-based superconductors, where nonmagnetic density functional calculations yield large errors in the structure relative to experiment, a fact that is thought to be related to the interplay between bonding and magnetism in those compounds.[22–29]

III. ELECTRONIC STRUCTURE

The electronic density of states (DOS) as obtained with the PBE GGA is shown in Fig. 1. The valence electronic structure is semiconducting and consists of a broad set of Ga derived sp bands starting at ~-11 eV with respect to the valence band maximum (VBM). A much narrower set of Fe d bands overlap these and extend from ~-2 to ~$+2$ eV with respect to the VBM. The Fe d derived part of the DOS (see Fig. 1) consists of narrow peaks and makes practically no contribution below ~-3 eV binding energy and certainly not near the bottom of
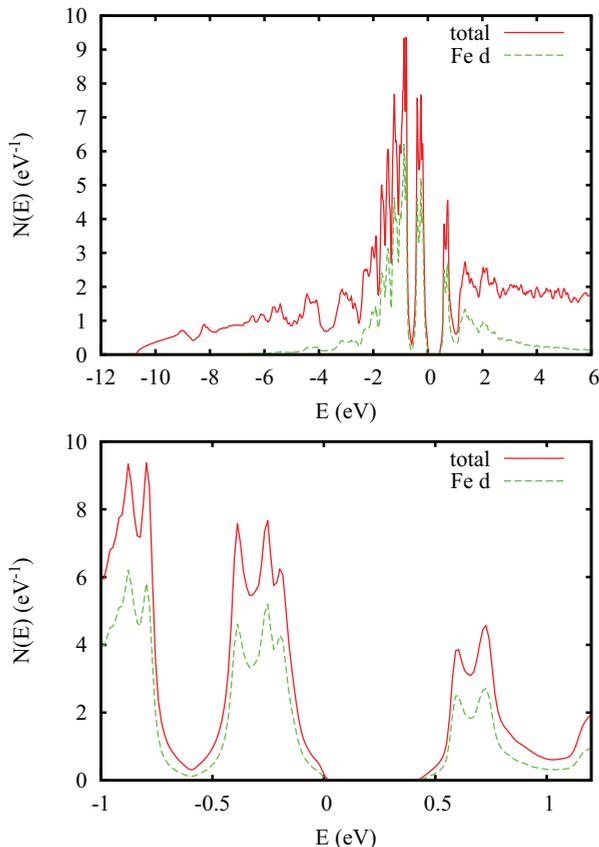

FIG. 1. (Color online) Calculated electronic density of states and Fe d projection onto the Fe LAPW sphere for FeGa$_3$ on a per formula unit basis. Spin orbit is included. (Bottom) A blow-up around the band gap.
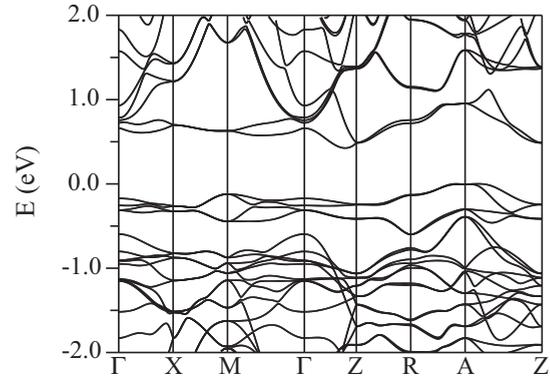

FIG. 2. Band structure of FeGa$_3$ including spin orbit as obtained with the PBE GGA.

the Ga sp bands, indicating relatively weak bonding between the Fe d and Ga sp systems.

The band structure in the energy region around the band edge is shown in Fig. 2. The calculated band gap is $E_g = 0.426$ eV including spin orbit and becomes only slightly larger (0.428 eV) if spin orbit is neglected. This small difference presumably reflects the fact that the states at the band edges come from very narrow ($\leqslant 0.5$ eV wide) Fe d bands with little Ga p contribution (spin orbit is stronger for p states than d states and for heavier atoms, i.e., Ga rather than Fe). It is also notable that the valence and conduction bands have different orbital characters. This is also seen in the calculations of Yin and Pickett.[12] The low site symmetry and the presence of interactions both between the Fe and Ga, as well as between the Fe atoms in the dimers leads to a mixing of the d orbitals. However, with the crystallographic setting above the conduction band minimum (CBM) has primarily z^2 orbital character, while the VBM has primarily $x^2 - y^2$ character.

Turning to the structure of the DOS, one notes that the DOS increases very rapidly away from the band edges reflecting the narrow bands and reaches high values well above 2 eV^{-1} on a per Fe basis. This suggests the possibility of a Stoner mechanism for itinerant ferromagnetism when doped. Such a steep density of states in a material that can be doped metallic is also favorable for obtaining high thermopowers at high doping levels. This is one ingredient in obtaining thermoelectric performance (the others are low lattice thermal conductivity and high mobility; the figure of merit is $ZT = \sigma S^2 T / \kappa$, where σ is the electrical conductivity, κ is the thermal conductivity, and S is the thermopower).

IV. FERMI SURFACES AND TRANSPORT

Before discussing the magnetism, we briefly mention the Fermi surface for doped material and the thermopower. Figure 3 shows the calculated Fermi surface for rigid band shifts of the Fermi energy, E_F, into the conduction and valence band edges. As may be seen, besides having different orbital character, the Fermi surfaces for hole and electron doped material are very different. For lightly electron doped material, the Fermi surface consists of a three-dimensional electron section near the Z point. At low carrier concentration, this is a pocket off the Z point along the Γ-Z direction

Hole Doped:
-0.04 eV   -0.08 eV   -0.12 eV   -0.16 eV

Electron Doped:
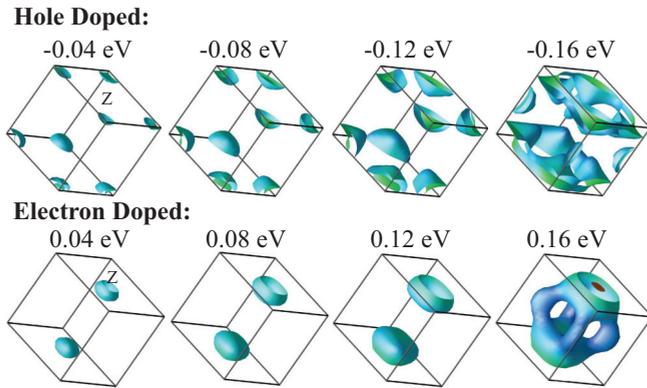0.04 eV   0.08 eV   0.12 eV   0.16 eV

FIG. 3. (Color online) Rigid band Fermi surface for shifts of E_F into the valence (top) or conduction (bottom) bands. The energies are E_F relative to the VBM or CBM, respectively. Spin orbit is included. The corresponding hole or electron counts in parenthesis on a per unit cell, four formula unit basis, are for hole doped, -0.16 eV (0.93), -0.12 eV (0.43), -0.08 eV (0.21), -0.04 eV (0.09) and for electron doped, 0.04 eV (0.03), 0.08 eV (0.08), 0.12 eV (0.17), and 0.16 eV (0.51).

corresponding to the CBM in Fig. 2. The two pockets on the opposite sides of the $k_z = 1/2$ zone boundary then merge to form the Z point pocket, which has a narrowing in the $k_z = 1/2$ plane as seen. The critical composition at which ferromagnetism is reported to start is at $x_c = 0.043$,[5] which corresponds to a band filling between the 0.08 and 0.12 eV plots of Fig. 3.

As the carrier density further increases, a second pocket develops around Z and the Fermi surface forms connections along the k_z direction, as shown in the bottom right panel of the figure. For higher carrier concentration (not shown), these connections merge to form a complex shaped cylinder while Z centered sections remain. Besides observing the complexity of the Fermi surface, one may note that it is clearly three dimensional with substantial dispersion in both the in-plane and k_z directions. This is in contrast to other well studied layered materials that may be near ferromagnetic quantum critical points, i.e., Na_xCoO_2,[30–34] and $Sr_3Ru_2O_7$.[35] The Fermi surfaces for hole doping are pockets around the A point. These connect in the $k_z = 0.5$ plane for higher doping levels. As seen, these are also very three dimensional.

The comparison of the electronic structure of the ordered cells and the virtual crystal with that of the stoichiometric compound, as discussed below, suggests that a rigid band model is reasonable for studying the transport. We calculated the doping dependent thermopower with a rigid band approximation and the constant scattering time approximation, similar to recent studies on thermoelectric materials.[36–38] The constant scattering time approximation consists of assuming that the energy dependence of the scattering rate at a given temperature and doping level is negligible on the scale of KT. It does not involve assumptions about the dependence of the scattering rate on either temperature or doping level, which can be strong. These calculations were done using the BOLTZTRAP code,[39] which employs a smooth interpolation of the energy bands on a fine grid to calculate band velocities and perform transport integrals. Importantly, the constant scattering time
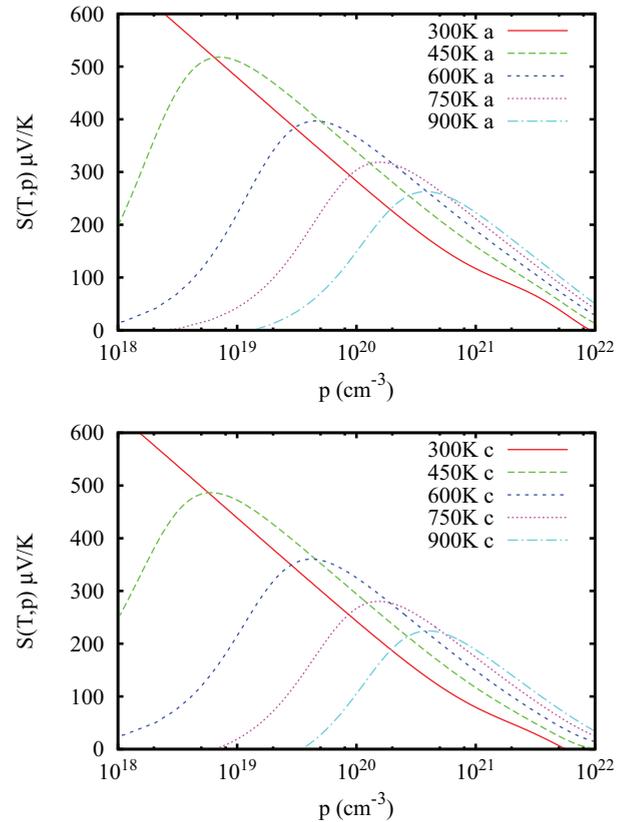

FIG. 4. (Color online) Calculated p-type $S(T)$, for in-plane (top) and c-axis (bottom) transport, as a function of carrier concentration, i.e., doping level.

approximation allows one to obtain first-principles results for the thermopower $S(T)$ without any adjustable parameters.

The calculated $S(T)$ for p-type and n-type $FeGa_3$ are shown in Figs. 4 and 5, respectively. As may be seen, the behavior is rather symmetric between p and n type in that high values of $S(T)$ are obtained at relatively high doping levels $\sim 10^{20}$ cm^{-3}. Also, the thermopower is rather isotropic as is typically but not always the case.[40]

Hadano and co-workers[3] obtained an n-type thermopower reaching ~ -350 μV/K at 300 K. In magnitude, this is below the highest magnitude of the thermopower at that temperature in our calculations. The inferred carrier concentration (i.e., doping level) is $n \sim 10^{19}$ cm^{-3} or slightly below, and the downturn at higher T is presumably due to bi-polar transport. Amagai and co-workers[2] obtained $S(300$ K$) = -563$ μV/K on a sample with a Hall carrier concentration of 3.1×10^{18} cm^{-3}. Taking the Hall concentration as the absolute carrier concentration, we obtain $S(300$ K$) = -480$ μV/K for this condition. Haldolaarachchige and co-workers[4] also reported high-room temperature values, though somewhat lower than those of Amagai and co-workers, on nominally stoichiometric $FeGa_3$, with a decrease upon doping with Co and Ge.

The magnitudes of $S(T)$ are relatively high compared to most semiconductors, reflecting the narrow bands around the band edges. These are sufficient that one might expect good thermoelectric performance in this compound if the doping level can be optimized and the other properties are favorable. In this regard the reported lattice thermal conductivity of
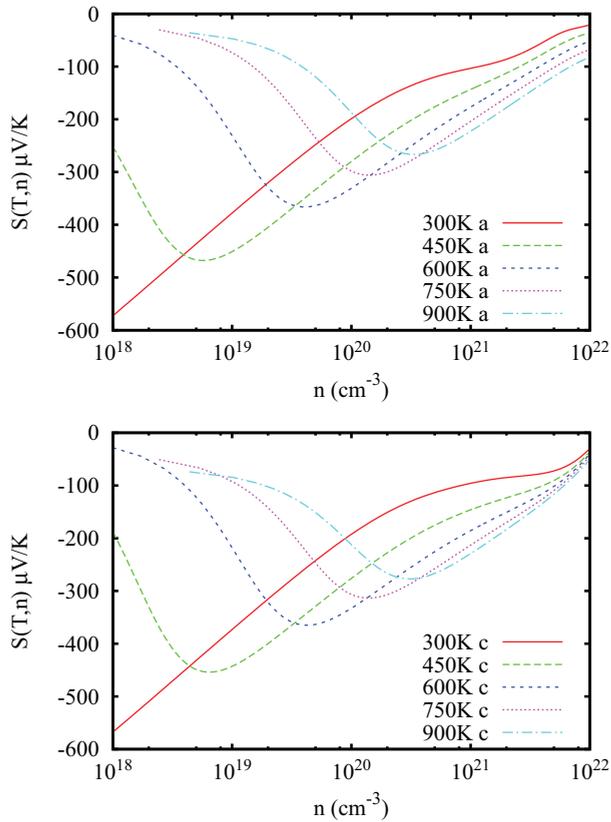
FIG. 5. (Color online) Calculated n-type $S(T)$, for in-plane (top) and c-axis (bottom) transport, as a function of carrier concentration, i.e., doping level.

FIG. 6. Total magnetic moment per formula unit as a function of composition for $Fe(Ga_{1-x}Ge_x)_3$ as obtained with the virtual crystal approximation including spin orbit. This figure is based on the total magnetization integrated over the whole unit cell. The moments inside the Fe LAPW spheres (radius 2.05 Bohr) account for $\sim 75\%$ of the magnetization.

FeGa$_3$ is 3.7 W/mK at 300 K and decreases to $\sim$2 W/mK at at 900 K.[2] These are reasonably low values consistent with a thermoelectric material that can be used at high T. We note that the T dependence suggests that some of the reported lattice thermal conductivity at high T could in fact have an origin in the bi-polar conduction. In any case, the thermal conductivity was observed to decrease with doping.[4] While the values of the experimental thermoelectric figures of merit reported to date are not high, the present results for the thermopower suggest that the best performance would be obtained at high T (750 K and above) with carrier concentrations (doping levels) of 3×10^{20}–1×10^{21} cm^{-3} for both p and n types. This is a regime for which thermoelectric properties have not been reported. It will be of interest to study samples in this range of carrier concentration (doping level) and temperature.

V. DOPING AND FERROMAGNETISM

We examined the possibility of itinerant Stoner ferromagnetism using direct calculations. These included virtual crystal calculations, with the virtual crystal approximation applied to the Ga site as well as supercell calculations in which a Ge atom was substituted on either the Ga1 or Ga2 sites in cell (i.e., $x_{Ge} = 1/12$). We also did calculations where one of the four Fe atoms in the unit cell was replaced by Co. In these calculations with partial substitution, we kept the lattice parameters fixed, but relaxed the atomic coordinates by total
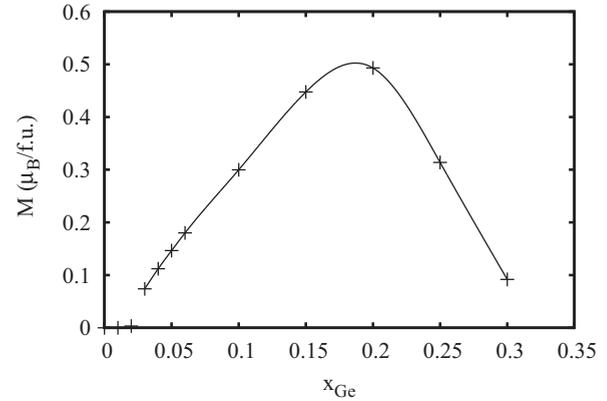
energy minimization. These three ordered cells all contain one electron per unit cell more than stoichiometric FeGa$_3$.

We start with the virtual crystal approximation, which allows for arbitrary doping levels. The main result is shown in Fig. 6. We find itinerant ferromagnetism starting at low doping levels, $\sim x_{Ge} = 0.03$. This becomes half-metallic almost immediately as the doping level is increased. This half-metallic ferromagnetic state persists up to $\sim x_{Ge} = 0.15$, after which the moment saturates and turns down above $\sim x_{Ge} = 0.2$, i.e., going over to an ordinary ferromagnetic metal. The ferromagnetism is lost near $x_{Ge} = 0.3$.

Half-metals are ferromagnets where one spin channel is semiconducting, while the other is metallic.[41–43] In such materials, spin-flip scattering is blocked and ferromagnetic domain walls can have high resistance, leading to unusual magnetotransport phenomena such as large negative magnetoresistance. Such materials are also of interest as "spintronic" materials, since their electrical transport is entirely in one spin channel, and also because the magnetic excitation spectrum is different than in ordinary metallic ferromagnets, in particular, as regards the Stoner continuum. In the present case, the majority spin channel is metallic while the minority spin is semiconducting. It is interesting to note that the calculated behavior regime is similar to that of the p-type material, Na$_x$CoO$_2$.[31] Na$_x$CoO$_2$ is also a good thermoelectric, whose high thermopower can be associated with narrow transition metal d bands.[44]

In any case, the behavior found is consistent with experimental reports.[5] The critical Ge concentration in experiment is reported to be $x_c = 0.043$, which is close to but above the calculated value. This is in contrast to standard density functional results for other quantum critical systems. In several of those cases, the magnetic state is overly stable relative to experiment, reflecting neglect of quantum critical fluctuations in standard density functional calculations.[31,45] This may imply that the magnitude of the critical fluctuations in $Fe(Ga_{1-x}Ge_x)_3$ are weaker than those in, e.g., Sr$_3$Ru$_2$O$_7$, which would imply a smaller region in temperature-composition (corresponding

$Fe(Ga_{0.9}Ge_{0.1})_3$
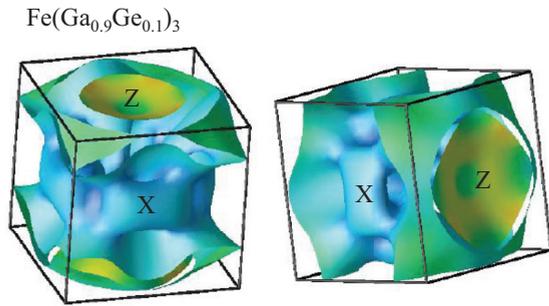

FIG. 7. (Color online) Calculated Fermi surface of virtual crystal ferromagnetic $Fe(Ga_{0.9}Ge_{0.1})_3$ as obtained with the PBE GGA, including spin orbit.

to temperature field in $Sr_3Ru_2O_7$) space showing quantum criticality associated with nearness to ferromagnetism.

The calculated Fermi surface for ferromagnetic $Fe(Ga_{0.9}Ge_{0.1})_3$ is shown in Fig. 7. The material is half-metallic at this composition. The composition corresponds to a charge of 1.2 additional electrons per unit cell relative to $FeGa_3$. Not surprisingly, the Fermi surface is large and complex for this high electron count. As mentioned, it is clearly not a two dimensional electron system. This illustrates the continuous evolution of the material with doping from a low carrier density ferromagnetic semiconductor to a half-metallic large Fermi surface metal.

It is not known how to heavily dope p-type in this compound. However, not surprisingly in view of the DOS, we also find in virtual crystal calculations that the compound will become a half-metallic ferromagnetic metal in this case. It will be of interest to investigate potential p-type dopants to determine whether a ferromagnetic quantum critical point can be obtained in this case as well.

As mentioned, calculations were also done for ordered cells. We find half-metallic ferromagnetism very similar to that in the virtual crystal case when one of the twelve Ga in the unit cell is replaced by Ge. The density of states is practically the same as in the virtual crystal calculation for this case. In the cell where one Fe was replaced by Co, we also find a density of states near the band edges that is similar to the undoped case and we find an upward shift of the Fermi energy into the conduction band. We find therefore that Co is an effective n-type dopant similar to Ge and that the Co-doped system shows near rigid band behavior. This is similar to what was found by Haussermann and co-workers for pure $CoGa_3$ in relation for $FeGa_3$[1] and is also in accord with the calculations of Verchenko and co-workers.[14] Consistent with this we obtain a half-metallic ferromagnetic state in this cell. This is in apparent disagreement with experiment, where it is reported that Co substitution does not produce ferromagnetism in any amount.[5] We do not know the reason for this disagreement. One possibility is that Co favors another magnetic order (not ferromagnetic). Another possibility is that alloy disorder on the Fe site induced by 25% Co replacement is sufficiently strong to destroy the ferromagnetism (this is neglected in our calculation, which uses an artificial perfect ordering of Fe and Co). Related to this, it is possible that the presence of Co-Co dimers in the alloy, but not in the present calculation affects the behavior. Finally, we note that Bittar and co-workers

observed that lower Co concentration $\sim 5\%$ substitution brings the system close to ferromagnetism based on the enhancement of the susceptibility.[7]

VI. PBE + U CALCULATIONS

As mentioned, a scenario in which semiconducting $FeGa_3$ is antiferromagnetic with pairs of Fe atoms forming singlets was proposed by Yin and Pickett[12] based on LDA + U calculations and subsequently criticized by Oscorio-Guillen and co-workers,[13] based on theoretical considerations. Arita and co-workers[46] used photoemission and inverse photoemission experiments to investigate the electronic structure. They find that the spectra can be reproduced by LDA + U calculations using values of U of ~ 3 eV. However, the density of states obtained is very similar between such calculations and $U = 0$ density functional calculations. The data in relation to the calculations do not clearly distinguish the LDA + U and $U = 0$ calculations, and as mentioned, there are some other questions that arise with an explanation in terms of an antiferromagnetic ground state. In any case, we did additional calculations with various values of U and different double counting schemes.

We start with calculations with the fully localized limit (SIC) double counting, similar to what was reported by Yin and Pickett. Our PBE + U calculations were done without spin orbit. First of all, we verified that there is no antiferromagnetic solution without U. Secondly, in calculations with the SIC double counting, we do find an antiferromagnetic solution in accord with what was reported by Yin and Pickett. We obtain a moment in the Fe LAPW sphere (radius 2.05 Bohr) of 0.52 μ_B with $U - J = 1.4$ eV, again in accord with Yin and Pickett (who, however, do not state the sphere radius over which they integrated the moment).

We also find that we can obtain an antiferromagnetic solution with the AMF double counting, but that substantially higher $U - J$ is needed. At $U - J = 3$ eV, the moment in the LAPW sphere is still only $0.39 \mu_B$. Also, we do not find good local moment behavior. Specifically, the moment vanishes for imposed ferromagnetic ordering with SIC double counting and $U - J = 1.4$ eV. This implies that U is stabilizing a band structure driven antiferromagnet, which is not consistent with the assumptions of the fully localized limit. We note that there is no clear justification for adding U in weak or moderately correlated transition metal compounds especially with this double counting scheme—a point that was emphasized by Oscorio-Guillen and co-workers.[13] For example, Fe metal is well described by standard density functionals, and agreement with experiment would be degraded if one performs $+U$ calculations.

In any case, at higher $U - J$, we do obtain behavior that is closer to local moment in the sense that both ferromagnetic and antiferromagnetic solutions can be found, but the moments are high at that point, and clearly should have been seen in the susceptibility if present. For $U - J = 3.0$ eV, we obtain a moment of $1.70 \mu_B$ for the antiferromagnetic order and 1.43 μ_B for ferromagnetic.

For the AMF double counting, while we do obtain an antiferromagnetic solution at $U - J = 3$ eV, we do not obtain a ferromagnetic solution. This provides a resolution for the apparent discrepancy between the results of Yin and Pickett

and those of Oscorio-Guillen and co-workers, who considered ferromagnetic ordering via fixed spin moment calculations.

Thus it is possible to obtain small antiferromagnetic moments with PBE + U calculations, but these are band structure related, inconsistent with the assumptions of the SIC double counting. At higher U, where local moments are found, these are large, approaching $2\mu_B$, inconsistent with experiment. We note that the use of SIC double counting LDA + U calculations with low values of $U - J$ is rarely justified. Clearly, it is not the case that there is a stable moment approximating spin 1/2 over a range of U. Rather, the value used by Yin and Pickett is a threshold value for the SIC double counting where the Fe begins a spin state transition and its moment rapidly increases with U. This means that models based on spin-1/2 Fe moments are not applicable for FeGa$_3$. Therefore there is not a good analogy with, e.g., the spin-1/2 VO$_2$ system, although we do note that the strong dependence of the moments on ordering found in PBE + U calculations, and the relatively large energies associated with this imply that there are strong band structure derived interactions between the Fe atoms in the dimers.

In any case, the present results raise doubts about whether there are such static moments in undoped FeGa$_3$. Furthermore, as discussed above, we can obtain ferromagnetism in doped FeGa$_3$ without assuming such pre-existing moments. Neutron diffraction measurements for semiconducting FeGa$_3$ should be sensitive to any ordered Fe moments if present, in particular, through symmetry lowering from the full $P4_2/mnm$ space group.

VII. SUMMARY AND CONCLUSIONS

In summary, we presented first-principles calculations of the electronic structure and transport properties of FeGa$_3$. We find that modest electron or hole doping can produce itinerant ferromagnetism in this compound. This does not depend on the presence of pre-formed moments in the undoped semiconducting phase. It will be of interest to search experimentally for moments and to examine the nature of the ferromagnetic phase in more detail. Itinerant magnetism implies strong coupling between the electrons at the Fermi energy that control transport and the magnetism. As such, FeGa$_3$ may be a particularly interesting material near a quantum critical point. We find that the ferromagnetic state is half-metallic over a substantial composition range. The results also show some promise as a thermoelectric material at high temperature if the doping level is optimized.

---

[1] U. Haussermann, M. Bostrum, P. Viklund, O. Rapp, and T. Bjornangen, J. Solid State Chem. **165**, 94 (2002).

[2] Y. Amagai, A. Yamamoto, T. Iida, and Y. Takanashi, J. Appl. Phys. **96**, 5644 (2004).

[3] Y. Hadano, S. Narazu, M. A. Avila, T. Onimaru, and T. Takabatake, J. Phys. Soc. Jpn. **78**, 013702 (2009).

[4] N. Haldolaarachchige, A. B. Karki, W. A. Phelan, Y. M. Xiong, R. Jin, and J. Y. Chan, J. Appl. Phys. **109**, 103712 (2011).

[5] K. Umeo, Y. Hadano, S. Narazu, T. Onimaru, M. A. Avila, and T. Takabatake, Phys. Rev. B **86**, 014421 (2012).

[6] N. Haldolaarachchige, J. Prestigiacomo, W. A. Phelan, Y. M. Xiong, G. McCandless, J. Y. Chan, J. F. DiTusa, I. Vekhter, S. Stadler, D. E. Sheehy, P. W. Adams, and D. P. Young, arXiv:1304.1897 [cond-mat].

[7] E. M. Bittar, C. Capan, G. Seyfarth, P. G. Pagliuso, and Z. Fisk, J. Phys.: Conf. Ser. **200**, 012014 (2010).

[8] V. G. Storchak, J. H. Brewer, R. L. Lichti, R. Hu, and C. Petrovic, J. Phys.: Condens. Matter **24**, 185601 (2012).

[9] R. S. Perry, L. M. Galvin, S. A. Grigera, L. Capogna, A. J. Schofield, A. P. Mackenzie, M. Chiao, S. R. Julian, S. I. Ikeda, S. Nakatsuji, Y. Maeno, and C. Pfleiderer, Phys. Rev. Lett. **86**, 2661 (2001).

[10] K. Huang, J. J. Hamlin, R. E. Baumbach, M. Janoschek, N. Kanchanavatee, D. A. Zocco, F. Ronning, and M. B. Maple, Phys. Rev. B **87**, 054513 (2013).

[11] Y. Imai and A. Watanabe, Intermetallics **14**, 722 (2006).

[12] Z. P. Yin and W. E. Pickett, Phys. Rev. B **82**, 155202 (2010).

[13] J. M. Osorio-Guillen, Y. D. Larrauri-Pizarro, and G. M. Dalpian, Phys. Rev. B **86**, 235202 (2012).

[14] V. Y. Verchenko, M. S. Likhanov, M. A. Kirsanova, A. A. Gippius, A. V. Trachev, N. E. Gervits, A. V. Galeeva, N. Buttgen, W. Kratschmer, C. S. Lue, K. S. Okhotnikov, and A. V. Shevelkov, J. Solid State Chem. **194**, 361 (2012).

[15] V. Eyert, Ann. Phys. **11**, 650 (2002).

[16] V. Eyert, Phys. Rev. Lett. **107**, 016401 (2011).

[17] N. Tsujii, H. Yamaoka, M. Matsunami, R. Eguchi, Y. Ishida, Y. Senba, H. Ohashi, S. Shin, T. Furubayashi, H. Abe, and H. Kitazawa, J. Phys. Soc. Jpn. **77**, 024705 (2008).

[18] Y. Takagiwa, K. Kitahara, Y. Matsubayashi, and K. Kimura, J. Appl. Phys. **111**, 123707 (2012).

[19] J. P. Perdew, K. Burke, and M. Ernzerhof, Phys. Rev. Lett. **77**, 3865 (1996).

[20] D. J. Singh and L. Nordstrom, *Planewaves Pseudopotentials and the LAPW Method*, 2nd ed. (Springer, Berlin, 2006).

[21] P. Blaha, K. Schwarz, G. Madsen, D. Kvasnicka, and J. Luitz, *wien2k, An Augmented Plane Wave + Local Orbitals Program for Calculating Crystal Properties* (K. Schwarz, Tech. Univ. Wien, Austria) (2001).

[22] J. Dong, H. J. Zhang, G. Xu, Z. Li, G. Li, W. Z. Hu, D. Wu, G. F. Chen, X. Dai, J. L. Luo, Z. Fang, and N. L. Wang, Europhys. Lett. **83**, 27006 (2008).

[23] S. Ishibashi, K. Terakura, and H. Hosono, J. Phys. Soc. Jpn. **77**, 053709 (2008).

[24] T. Yildirim, Phys. Rev. Lett. **101**, 057010 (2008).

[25] Z. P. Yin, S. Lebegue, M. J. Han, B. P. Neal, S. Y. Savrasov, and W. E. Pickett, Phys. Rev. Lett. **101**, 047001 (2008).

[26] I. I. Mazin, M. D. Johannes, L. Boeri, K. Koepernik, and D. J. Singh, Phys. Rev. B **78**, 085104 (2008).

[27] I. I. Mazin, D. J. Singh, M. D. Johannes, and M.-H. Du, Phys. Rev. Lett. **101**, 057003 (2008).

[28] F. Bondino, E. Magnano, M. Malvestuto, F. Parmigiani, M. A. McGuire, A. S. Sefat, B. C. Sales, R. Jin, D. Mandrus, E. W. Plummer, D. J. Singh, and N. Mannella, Phys. Rev. Lett. **101**, 267001 (2008).

[29] D. C. Johnson, Adv. Phys. **59**, 803 (2010).

[30] D. J. Singh, Phys. Rev. B **61**, 13397 (2000).

[31] D. J. Singh, Phys. Rev. B **68**, 020503(R) (2003).

[32] L. M. Helme, A. T. Boothroyd, R. Coldea, D. Prabhakaran, D. A. Tennant, A. Hiess, and J. Kulda, Phys. Rev. Lett. **94**, 157206 (2005).

[33] S. P. Bayrakci, I. Mirebeau, P. Bourges, Y. Sidis, M. Enderle, J. Mesot, D. P. Chen, C. T. Lin, and B. Keimer, Phys. Rev. Lett. **94**, 157205 (2005).

[34] G. Cao, M. M. Korshunov, Y. Gao, M. Le Tacon, D. J. Singh, and C. Lin, Phys. Rev. Lett. **108**, 236401 (2012).

[35] S. A. Grigera, R. S. Perry, A. J. Schofield, M. Chiao, S. R. Julian, G. G. Lonzarich, S. I. Ikeda, Y. Maeno, A. J. Millis, and A. P. Mackenzie, Science **294**, 329 (2001).

[36] D. Parker and D. J. Singh, Phys. Rev. X **1**, 021005 (2011).

[37] D. J. Singh, Phys. Rev. B **81**, 195217 (2010).

[38] X. Chen, D. Parker, M. H. Du, and D. J. Singh, New J. Phys. **15**, 043029 (2013).

[39] G. K. H. Madsen and D. J. Singh, Comput. Phys. Commun. **175**, 67 (2006).

[40] K. P. Ong, D. J. Singh, and P. Wu, Phys. Rev. Lett. **104**, 176601 (2010).

[41] R. A. de Groot, F. M. Mueller, P. G. van Engen, and K. H. J. Buschow, Phys. Rev. Lett. **50**, 2024 (1983).

[42] J. M. D. Coey and M. Venkatesan, J. Appl. Phys. **91**, 8345 (2002).

[43] G. M. Muller, J. Walowski, M. Djordjevic, G. X. Miao, A. Gupta, A. V. Ramos, K. Gehrke, V. Moshnyaga, K. Samwer, J. Schmalhorst, A. Thomas, A. Hutten, G. Reiss, J. S. Moodera, and M. Munzenberg, Nat. Mater. **8**, 56 (2009).

[44] H. J. Xiang and D. J. Singh, Phys. Rev. B **76**, 195111 (2007)

[45] T. Moriya, *Spin Fluctuations in Itinerant Electron Magnetism* (Springer, Berlin, 1985).

[46] M. Arita, K. Shimada, Y. Utsumi, O. Morimoto, H. Sato, H. Namatame, M. Taniguchi, Y. Hadano, and T. Takabatake, Phys. Rev. B **83**, 245116 (2011).